

Supporting Information

**Resolving the Dynamic Properties of Entangled Linear Polymer
in Non-equilibrium Coarse Grain Simulation with *a priori* Scaling
Factor**

Yihan Nie^{1,2}, *Zhuoqun Zheng*³, *Chengkai Li*¹, *Haifei Zhan*^{2,1,4*}, *Liangzhi Kou*^{1,4}, *Yuantong
Gu*^{1,4*} and *Chaofeng Lü*^{5,2}

¹School of Mechanical, Medical and Process Engineering, Queensland University of
Technology (QUT), Brisbane QLD 4001, Australia

²College of Civil Engineering and Architecture, Zhejiang University, Hangzhou 310058,
China

³Center for Materials Science, Queensland University of Technology (QUT), Brisbane,
Queensland 4001, Australia

⁴School of Astronautics, Nanjing University of Aeronautics and Astronautics, Nanjing
210016, China

⁵Faculty of Mechanical Engineering & Mechanics, Ningbo University, Ningbo 315211, P.R.
China

S1 Structural distribution functions for the IBI, LIBI, and HIBI in 2BD and 1BD model

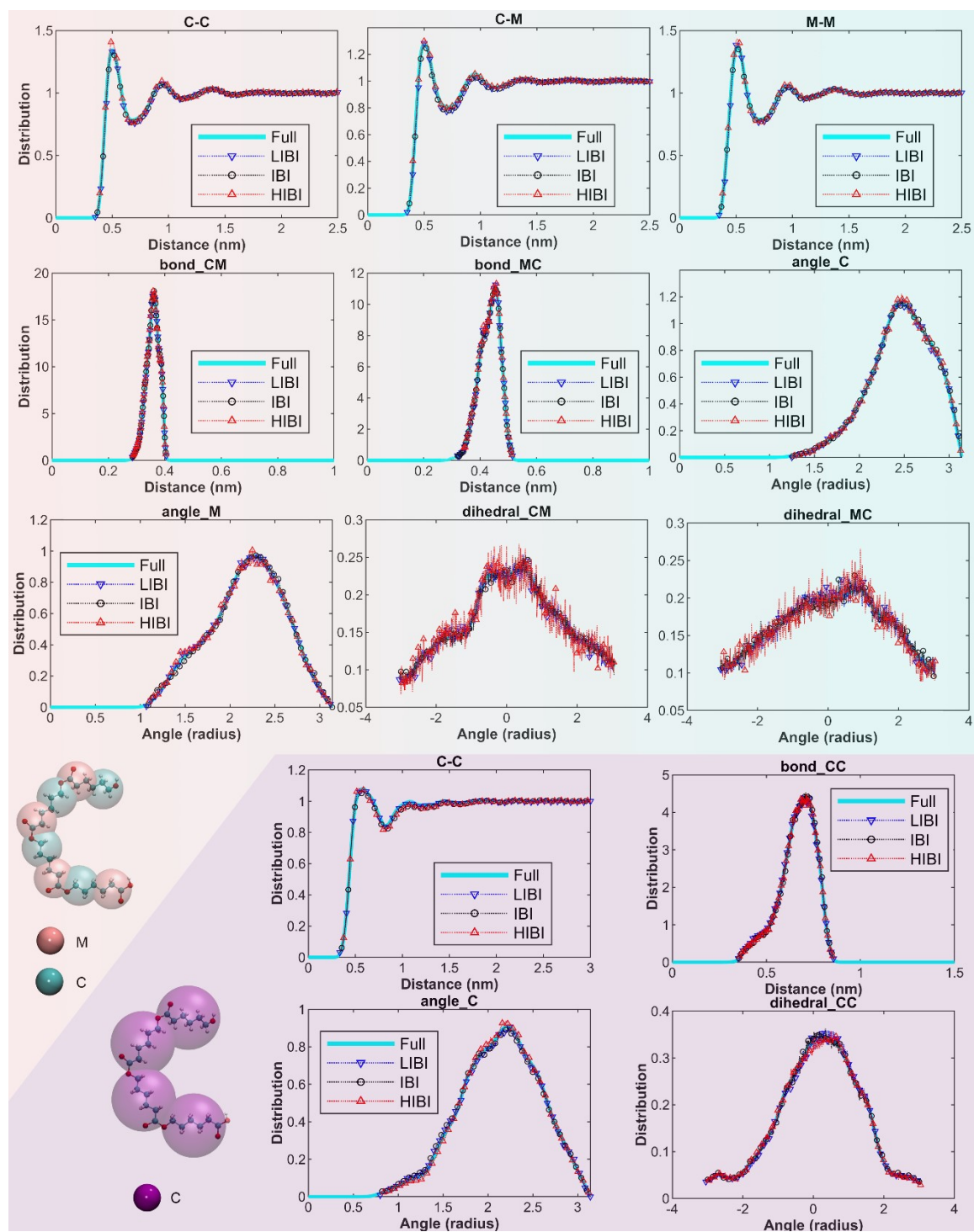


Figure S1 The distribution functions predicted by the IBI, LIBI and HIBI can match well with the full-atomic results in 2BD and 1BD models.

S2 Structural distribution functions for EIBI.

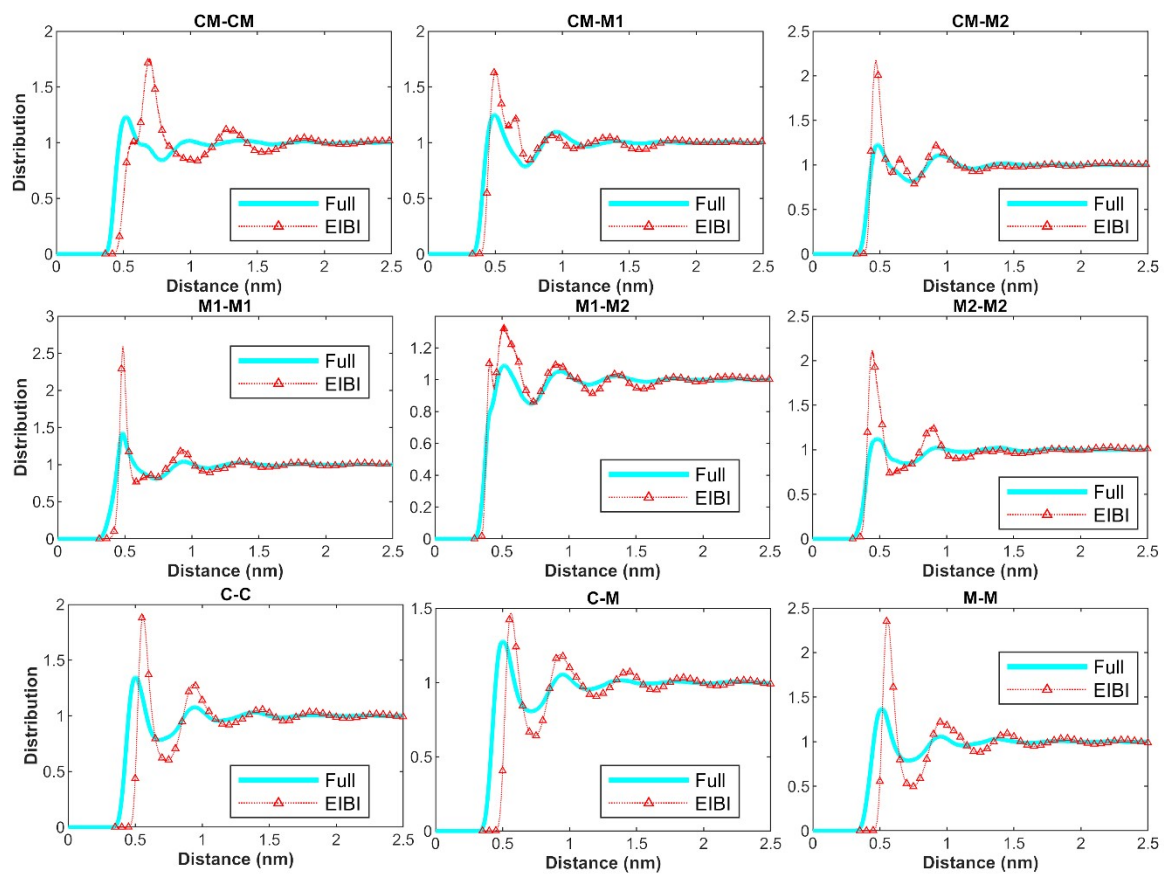


Figure S2 The structural distribution functions in 2BD and 3BD models with EIBI potential.

S3 Structural distribution functions for the DPD thermostat in 3BD model

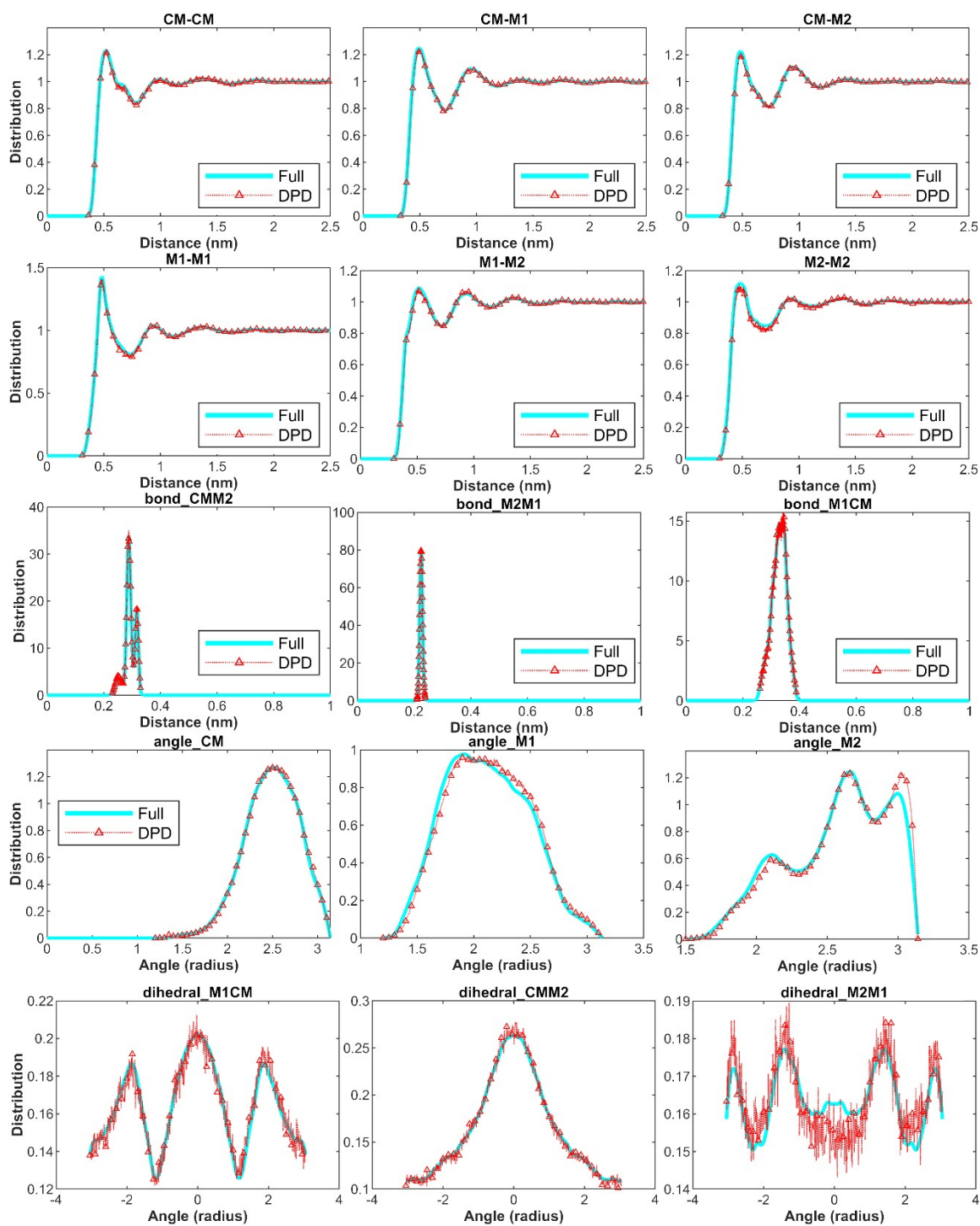


Figure S3 The structural distribution functions in 3BD model with IBI potential and DPD thermostat.

S4 Structural distribution functions for the DPD thermostat in 2BD and 1BD model

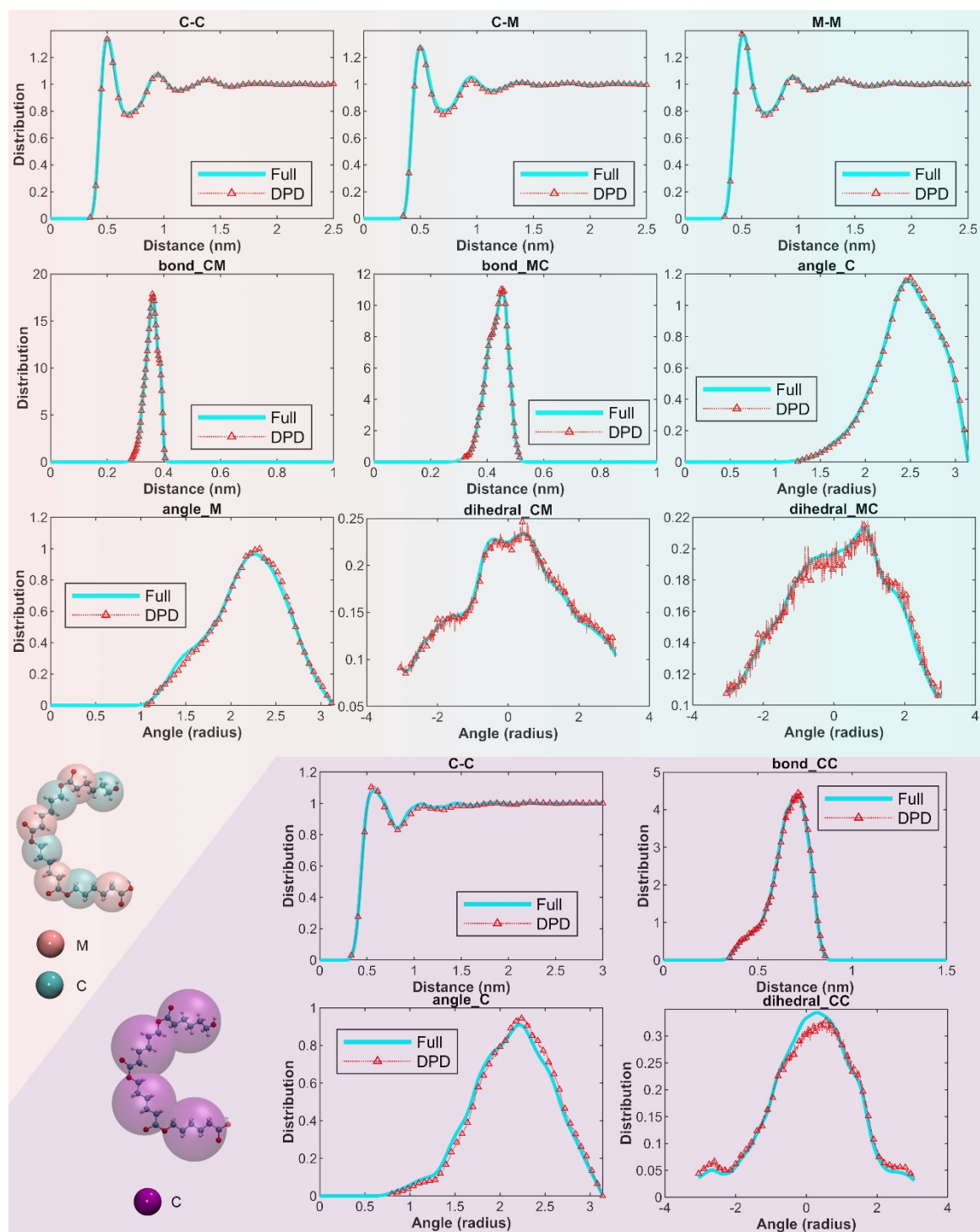


Figure S4 The structural distribution functions in 2BD and 1BD model with IBI potential and DPD thermostat.

S5 Mean squared displacement curves during the relaxation.

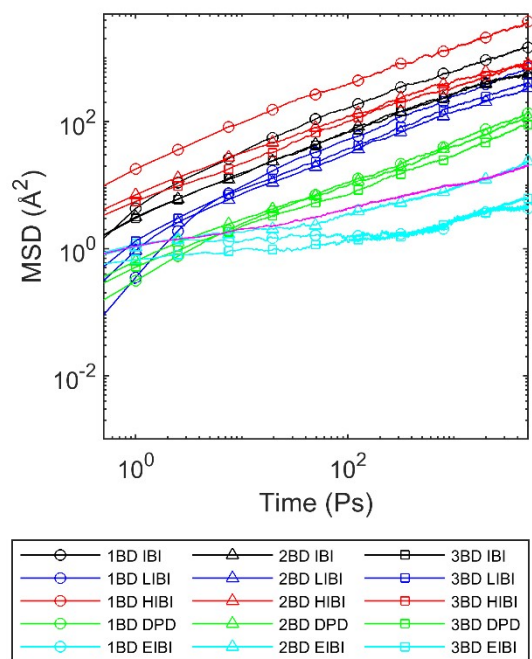


Figure S5 The MSD curves of the atoms and CG beads for different models.

S6 Enthalpy at different temperatures in different CG models

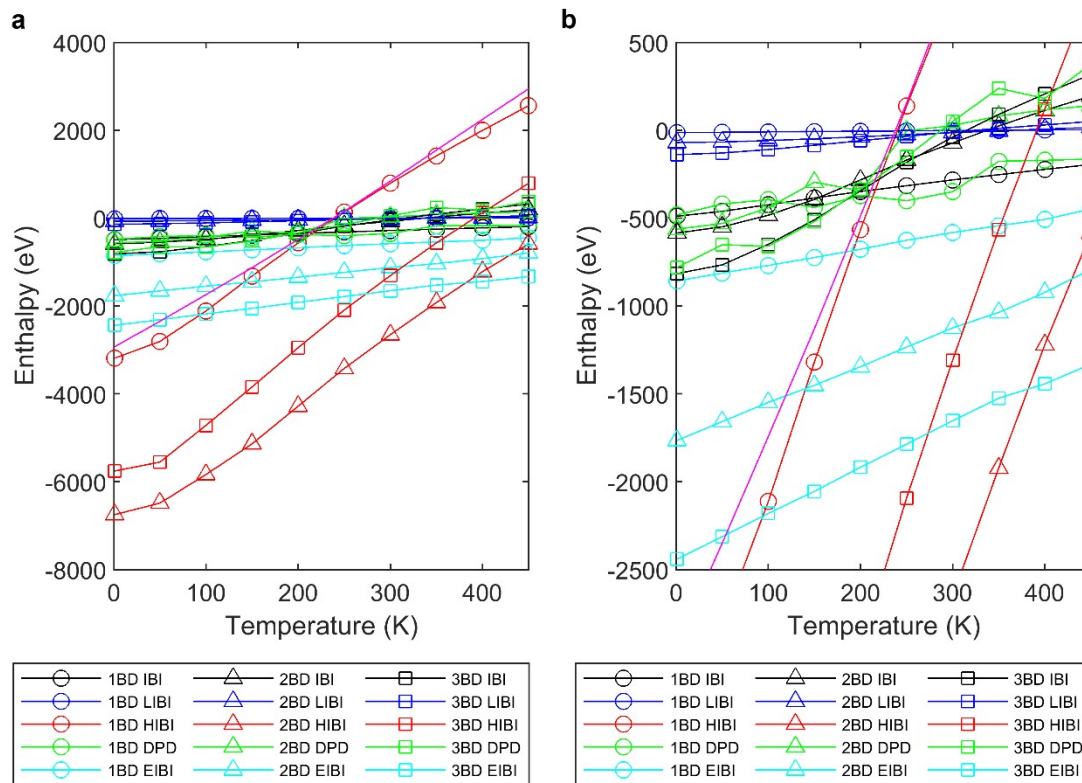


Figure S6 For the DPD model, as the non-conservative force is added, the pressure has a larger fluctuation than the IBI with the Nose-Hoover thermostat, which results in a larger fluctuation in enthalpy, but the value is close to IBI results on average. As for the EIBI method, the enthalpy is lower than that of the IBI results.

S7 Young's modulus at different strain rates in different CG models

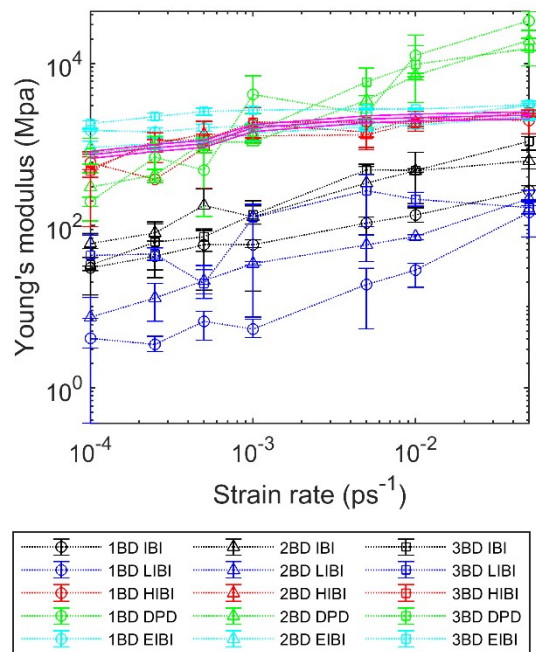


Figure S7 The Young's modulus in different CG models with different strain rates. The error bar shows the variance from the tensile tests in the three orthogonal directions for each model.

S8 The stress- strain curves for each model under different tensile rates.

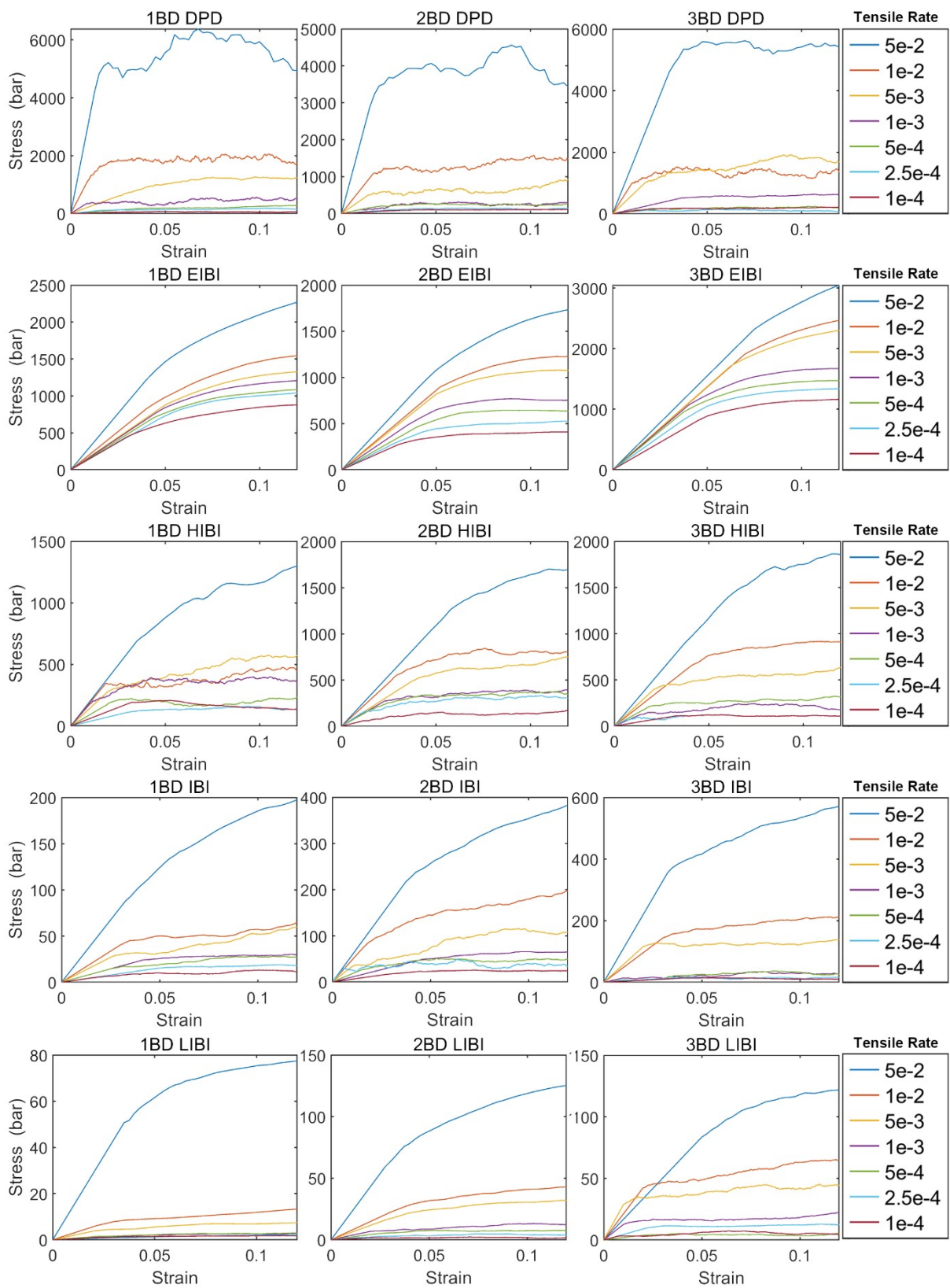


Figure S8 The stress-strain curve for each model under different tensile rates. The stress-strain curve is the averaged result from the tensile test in three directions.